

# Top and W Mass Measurements at the Tevatron

J. S. Miller

University of Michigan, Ann Arbor, MI 48109, USA

We describe measurements of the top quark and W boson masses with the CDF and D0 detectors at the Tevatron collider. We highlight the major features for the W mass measurement and present the Run 1 results. We present several different techniques used to measure the top quark mass and give recent results from D0 and CDF.

## 1. INTRODUCTION

In the Standard Model, the W mass can be directly related to the Z mass, the Fermi constant  $G_F$  and the electromagnetic coupling  $\alpha$ . These parameters are precisely measured and comparing the measured W mass to the prediction based on the other parameters provides an important test of the Standard Model. At the current level of precision, radiative effects which change the mass of the W are also important to consider. In particular, virtual top quark and Higgs boson effects in loop diagrams can shift the W mass. Since the Higgs mass is unknown, the measured top and W masses can be used to constrain the Higgs mass based on its contribution to the radiative correction. However, the dependence of the W mass shift on the Higgs mass is a logarithmic correction and thus only a loose constraint on the Higgs mass can be derived. Figure 1 shows the relation of the Higgs mass prediction to the W and top mass measurements using the precision electroweak data.

The top mass is not predicted in the Standard Model, but it is the most massive particle known, which motivates a good understanding of its properties. In addition, the top quark makes an important contribution to the radiative corrections of a number of electroweak observables, and a precise measurement of the top mass can be used with electroweak observables to constrain any new physics which might provide additional radiative corrections. A more detailed treatment of the relation between electroweak observables and the top and W masses is given in [1].

The CDF and D0 are both general purpose experiments operating at the Tevatron collider at Fermilab. The experiments took data from 1992-1995 and collected approximately  $110 \text{ pb}^{-1}$  of integrated luminosity. This is referred to as Run 1. During this time both experiments discovered the top quark and made a number of measurements related to the top quark and W boson. Since that time, both the CDF and D0 detectors had significant upgrades including new tracking chambers and all new electronics for triggering and data acquisition. These detectors are described in detail elsewhere [2, 3]. The data taking period beginning in 2001 with the upgraded detectors is referred to as Run 2. The Tevatron has delivered over  $600 \text{ pb}^{-1}$  of data and the dataset should substantially increase over the next few years.

In this paper I review measurements of the W boson and top quark masses with the CDF and D0 experiments. I first describe the experimental technique for measuring the W boson mass, the limiting systematic errors on the measurement and the methods for reducing them. I also review the CDF and D0 W mass measurements from Run 1. I then describe the several approaches used to measuring the top quark mass and the dominant systematic errors. I describe the result from a recent D0 top mass measurement based on Run 1 data and several preliminary Run 2 results from CDF on the top quark mass.

## 2. W MASS MEASUREMENT

### 2.1. Event Selection and Reconstruction

The W boson mass is measured with a sample of events where the W decays to either an electron or muon and its associated neutrino. The charged lepton must have a transverse momentum greater than  $25 \text{ GeV}/c$  and the missing transverse momentum due to the neutrino must also be greater than  $25 \text{ GeV}/c$ . Electrons are identified by a well

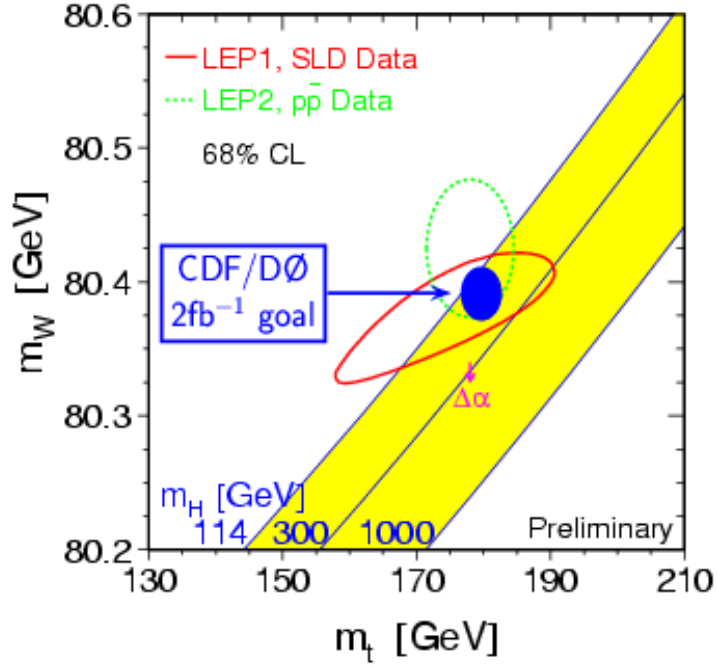


Figure 1: Direct measurements of the top and W mass can be combined with precision electroweak measurements to constrain the allowed values for the Higgs mass. The dotted contour is from the direct measurements of the top and W masses. The solid contour is the indirect estimates from precision electroweak fits, and the shaded diagonal region shows the Higgs mass prediction based on the measured top and W masses.

contained cluster of energy in the electromagnetic calorimeter with a track pointing to the cluster. In addition, only a small fraction of the electron energy can be contained in the hadronic part of the calorimeter. Muons are identified by a high momentum track pointing to hits in the muon detectors, and with the energy deposited by the track in the calorimeter consistent with a minimum ionizing particle. The identification of the electron or muon is also the basis of the trigger selection for the event sample.

The transverse momentum of the hadronic recoil opposite the W is based on the vector sum of the energy in all of the calorimeter towers not containing the lepton. The transverse neutrino momentum is inferred to be opposite the vector sum of the lepton and hadronic recoil transverse momenta. The total transverse recoil momentum is required to be less than 20 GeV/c. This removes events with significant hadronic activity which are more likely to be background events and for which the recoil momentum is likely to be less well measured.

The z component of the neutrino momentum is not measured because of the significant momentum carried by the proton and anti-proton remnants down the beam pipe. This prevents a direct reconstruction of the W mass. Instead we reconstruct the transverse W mass using the transverse momenta of the charged lepton and neutrino. We define the transverse mass as

$$M_T = \sqrt{2p_T^\ell p_T^\nu (1 - \cos\phi_{\ell\nu})}, \quad (1)$$

where  $\cos\phi_{\ell\nu}$  is the angle between the lepton and neutrino in the transverse plane. This gives a Jacobian peak with an edge at the W mass, but with the bulk of the distribution below the W mass from events with lepton momentum along the z direction. There is also a long tail above the W mass which arises from the 2 GeV width of the W. The precision with which the Jacobian edge can be reconstructed determines the precision of the W mass measurement. This reconstruction is limited by uncertainties in the hadronic recoil measured by the calorimeter which sets the uncertainty on the transverse neutrino momentum. Figure 2 illustrates the Jacobian peak of the transverse mass distribution.

The transverse momentum of the charged lepton by itself also gives a Jacobian peak with an edge at half of the

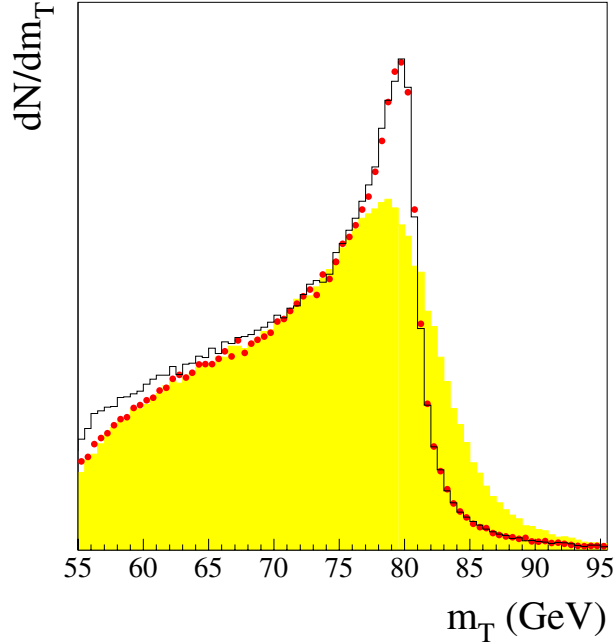


Figure 2: The W transverse mass distribution from simulation. The solid line is generated with the W  $p_T = 0$ , the points use the correct  $p_T$  distribution, and the shaded area includes the effects of detector resolution [4].

W mass. This has the advantage of just using the charged lepton momentum which is the best measured quantity in the event, and avoiding the uncertainty associated with reconstructing the neutrino. However, relating the charged lepton momentum to the W mass requires an understanding of the transverse momentum distribution of the W. This introduces an uncertainty based on the theoretical modeling of the W  $p_T$  distribution. In contrast, the transverse mass distribution is to first order insensitive to the transverse momentum of the W. Figures 3 and 2 illustrate the tradeoffs in the understanding of the W  $p_T$  spectrum and the neutrino measurement resolution.

## 2.2. Energy Scale Calibration

Measuring the W mass requires an absolute calibration of the energy and momentum scale of the detector. Understanding this scale has been the dominant systematic error for the W mass measurement and is ultimately limited by the size of the control samples used to set the scale.

A sample of  $J/\psi \rightarrow \mu^+\mu^-$ ,  $\Upsilon(1S) \rightarrow \mu^+\mu^-$ , and  $Z \rightarrow \mu^+\mu^-$  events are used to set the momentum scale for charged particle tracking. The large statistics  $J/\psi \rightarrow \mu^+\mu^-$  sample sets the momentum scale. Studying the momentum scale dependence on the polar angle of the track gives the track curvature correction as a function of polar angle. The momentum scale dependence on the track momentum is sensitive to the ionization energy loss and is used for calibration of the MC for material in the detector. The  $\Upsilon(1S) \rightarrow \mu^+\mu^-$  sample provides a check of the momentum scale at 10 GeV/ $c^2$  which is intermediate to the mass scale of the W and Z at 80 and 90 GeV/ $c^2$ , and the 3 GeV/ $c^2$  mass of the  $J/\psi$ . The  $Z \rightarrow \mu^+\mu^-$  sample provides a check of the momentum scale at the high mass scale. The fit to the width of the Z provides a measurement of the track resolution at that momentum which is used to tune the MC simulation. Figure 4 shows the CDF  $Z \rightarrow \mu^+\mu^-$  sample used for the Run 2 W mass analysis.

With the track momentum scale set using  $J/\psi$  decays, the electromagnetic calorimeter energy scale can be set using the peak of the  $E/p$  distribution for  $W \rightarrow e\nu$  decays, where  $E$  is the electromagnetic energy of the electron

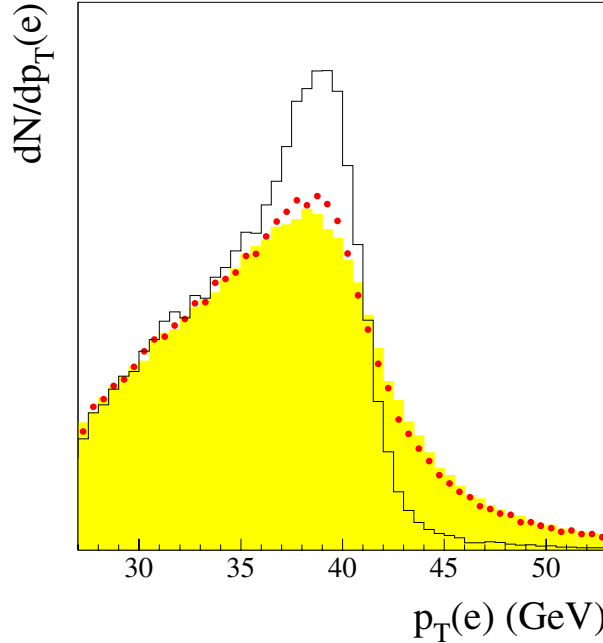


Figure 3: The lepton transverse momentum in W decays. The solid line is generated with the W  $p_T = 0$ , the points use the correct  $p_T$  distribution, and the shaded area includes the effects of detector resolution [4].

measured in the calorimeter and  $p$  is the momentum of the electron track. The width of the distribution near the peak is used to measure the energy resolution. The energy scale and resolution is also measured using a  $Z \rightarrow e^+e^-$  sample, which was the method used by CDF and D0 for the Run 1 measurements.

### 2.3. Backgrounds

The W sample has a background contamination from several sources. For  $W \rightarrow \mu\nu$ , the largest background is  $Z \rightarrow \mu\mu$  events where one of the muons is not reconstructed. The missing track also gives a momentum imbalance, allowing the event to pass the selection requirement for missing transverse momentum. This background is estimated using a MC sample to determine the fraction of Z events which pass the W selection cuts and normalized to the known ratio of W to Z production. These events are about 4% of the sample and MC events are used to model the shape of this background. For the  $W \rightarrow e\nu$  sample,  $Z \rightarrow ee$  contamination is estimated in the same way and is less than half a percent.

Another background comes from  $W \rightarrow \tau\nu$  events with the subsequent decay of the tau to an electron or muon. These events are indistinguishable from signal events, but have a softer lepton momentum spectrum. Again a MC sample is used to measure the efficiency and shape for reconstructing these events and the background is normalized to the known W cross section and leptonic branching fractions. The  $W \rightarrow \tau\nu$  events are 1-2% of the sample.

QCD background events are from jets which fake a lepton and also have a transverse momentum imbalance due to mismeasured jet energies. For most events with fake leptons, the lepton is not isolated from a jet and contains significant energy in a cone around the lepton. In addition, most of these events do not have a momentum imbalance. This background is estimated using events with either low momentum imbalance or non-isolated leptons to extrapolate into the signal region. The sideband events also give the kinematic shape of the background. The QCD background is about 1% of the sample.

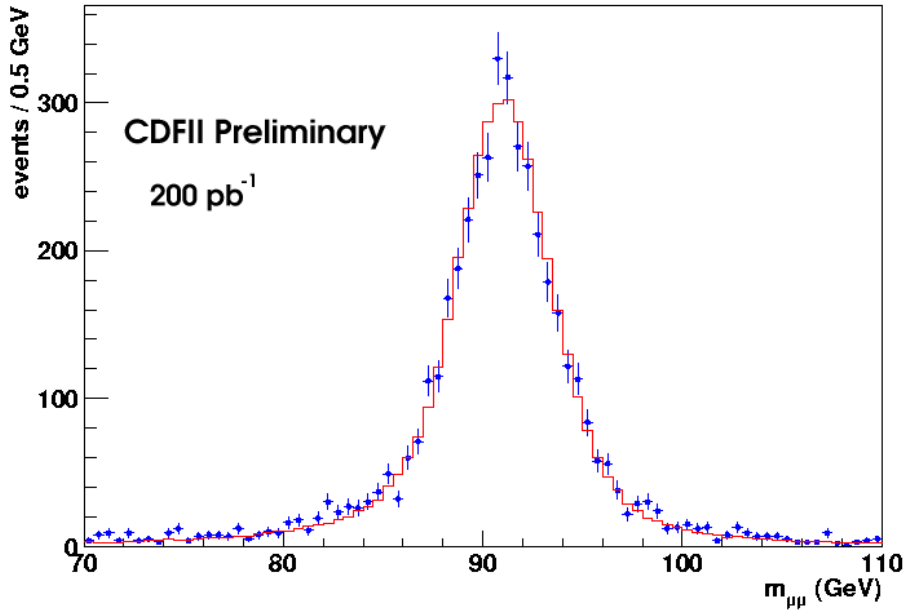


Figure 4: The reconstructed Z boson mass in the dimuon channel. The points are the data and the solid line is the simulation. The  $Z \rightarrow \mu\mu$  and  $Z \rightarrow ee$  samples set the momentum and energy scales and resolutions. The size of these samples largely determines the systematic error of the W mass measurement.

The muon channel has two additional backgrounds. One of these is kaon decays in flight which gives a real muon. If the kaon and muon tracks are sufficiently aligned, they will be reconstructed as a single track although with typically a larger  $\chi^2$  for the track fit parameters and a larger impact parameter. Using the track  $\chi^2$  and d0 distributions in the sample, this background is measured to be about 4% of the sample. Another muon specific background is due to cosmic rays which pass through the center of the detector at a time that overlaps with a beam crossing. Most of these events are rejected by the poor match of the tracking hit times with the beam crossing time, but a residual background at the level of a small fraction of a percent remains.

Both the normalization and the kinematic shape of the background contribute to the uncertainty on the W mass measurement. For each background source the normalization and shape of the lepton  $P_T$  and transverse W mass are varied to measure the systematic uncertainty. For all of the backgrounds the lepton momentum and transverse mass distributions are softer than the signal and do not rapidly vary near the Jacobian peak. Thus the backgrounds are not the limiting systematic for the measurement.

## 2.4. Signal Modeling

The W mass measurement depends critically on modelling W production and decay and the detector response to W events. The critical pieces are the  $p_T$  spectrum and rapidity distribution of the W, QED radiation in the decay, and the response of the detector to the hadronic recoil.

The W  $p_T$  comes from QCD radiation in the event. This includes both perturbative contributions at large W  $p_T$  and non-perturbative effects at low  $p_T$ . Because of the cut on the total hadronic recoil momentum, the W events used for the mass measurement are primarily at low  $p_T$ . The non-perturbative contributions are calculated using resummation techniques [8, 9] which relate the  $p_T$  distribution in Z and W events. For Run 2, CDF is using the RESBOS generator [7] with its parameters describing the non-perturbative physics tuned from fits of the Z  $p_T$  distribution. The W mass measurement based on the lepton  $p_T$  is more sensitive to the W  $p_T$  distribution than the

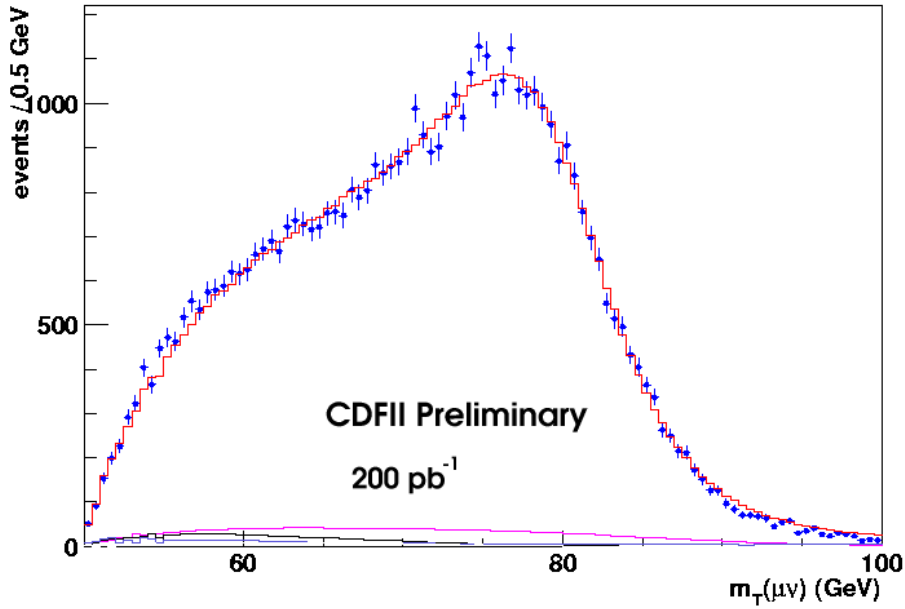


Figure 5: The transverse W mass for W decays to a muon and neutrino. The points are the data and the solid line is the simulation.

measurement based on the transverse mass.

Another generator level uncertainty is the parton distribution function (PDF) used by the event generator. Because of the acceptance cuts, the kinematic variables used for the measurement are not entirely invariant under a boost along the longitudinal direction. PDF distributions based on global fits to data are provided by the MRST [13] and CTEQ [14] groups. Changing the W production model based on variations of the PDF distributions provides an additional systematic on the W mass. This systematic can be reduced by including W events with leptons in the forward part of the detector to cover a larger range in rapidity as was done by D0 in Run 1 [5].

The leptons produced in the W decay can emit QED radiation which if unaccounted for would lead to shifts in the W mass of order  $100 \text{ MeV}/c^2$ . Most photons radiated from the lepton are collinear with the lepton. Those from electrons will shower in the same tower as the electron with no resulting loss in the electron energy measurement. Collinear photons associated with muons give a reduction in the measured muon momentum. Large angle QED radiation will have the same effect for electrons and muons. QED radiation is included in the generator as part of the W decay [10–12]. The current calculation only accounts for one additional photon. The effect of not including a second photon is a relatively small systematic.

A fast simulation is used to model the detector response to the lepton and hadronic recoil. The lepton resolution and energy loss in the detector is modelled based on detector calibrations described earlier. The response of the detector to the hadronic recoil is tuned using  $Z \rightarrow \ell\ell$  events, with the  $p_T$  of the Z used to tune the  $p_T$  balance and measure the resolution. The hadronic activity depends on both a hard component of the recoil and a soft component due to multiple interactions and the underlying event from the rest of the proton-anti-proton interaction. The detector model is then compared to the observed recoil spectrum for the W sample in Figure 5.

## 2.5. W Mass Results

The W mass was measured by both the CDF and D0 experiments in Run 1. D0 measured the W mass in the electron channel and obtained a result of  $80.483 \pm 0.084 \text{ GeV}/c^2$  [5]. CDF measured the W mass in both the muon

Table I: Run I W mass measurement uncertainties

Uncertainty (MeV)	CDF $\mu$	CDF $e$	D0 $e$
W statistics	100	65	60
Lepton energy scale	85	75	56
Lepton resolution	20	25	19
Recoil model	35	37	35
$p_T(W)$	20	15	15
Selection bias	18	-	12
Backgrounds	25	5	9
PDF's	15	15	8
QED radiative corr.	11	11	12
$\Gamma(W)$	10	10	10

and electron channels and obtained a combined result of  $80.433 \pm 0.079 \text{ GeV}/c^2$  [6].

The systematic errors are for the most part limited by the size of the sample of Z bosons used to calibrate the lepton energy scale, the W  $p_T$  distribution and the detector response to the hadronic recoil. The summary of errors from the CDF and D0 Run 1 measurements are given in Table I. With the increasing datasets for CDF and D0 for Run 2, the W and Z samples will increase leading to reduced statistical and systematic errors. At this time, there are no Run 2 W mass measurements from the Tevatron, but the expected error for  $2 \text{ fb}^{-1}$  of data is  $40 \text{ MeV}/c^2$  per experiment.

### 3. TOP MASS MEASUREMENTS

#### 3.1. Event Selection and Backgrounds

Top quark pair production in proton anti-proton collisions are produced through quark anti-quark annihilation and gluon-gluon fusion. At the Tevatron with a center of mass energy of 1.96 TeV the  $t\bar{t}$  production cross section is predicted to be 6.7 pb. Each top quark decays into a b quark and W boson, and the events can be classified by the decays of the W. Figure 6 illustrates  $t\bar{t}$  production and decay. Around 30% of the events have one of the W bosons decaying to an electron or muon and its associated neutrino, with the other W decaying into quark pairs which form hadronic jets. This lepton+jets mode is the dominant one used for the top mass measurement and will be the focus of this paper. Both W's decay to electrons or muons 5% of the time. This mode has very low background, but the size of the signal samples are significantly smaller. In addition, the presence of two undetected neutrinos complicates the event reconstruction. However, the dilepton sample is also used for the mass measurement. The all hadronic channel occurs 44% of the time and is when both W's decay to quark pairs, giving six jet events. This sample can also be used for a mass measurement, but is complicated by the large background from direct QCD jet production. The rest of  $t\bar{t}$  events are classified by when at least one of the W's decays to a  $\tau$  lepton.

$t\bar{t}$  events in the lepton plus jets mode are typically selected by requiring an isolated electron or muon with transverse momentum greater than 20 GeV/c, missing transverse momentum greater than 20 GeV/c plus the presence of 3 or more jets with transverse energy,  $E_T > 15 \text{ GeV}$  and a pseudorapidity  $|\eta| < 2$ . The pseudorapidity is defined as  $\eta = -\ln(\tan(\theta/2))$ , where  $\theta$  is the polar angle with respect to the beam direction. This sample is used for the top pair cross section measurements.

The dominant background in the lepton+jets sample is direct W production in association with jets. However, this background can be reduced by exploiting the fact that every top event will have b quark jets. These jets can be identified 30-40% of the time by finding a displaced secondary vertex inside the jet due to the relatively long lifetime of b hadrons. The efficiency to tag one or more jets in a  $t\bar{t}$  event is over 50% because each event typically

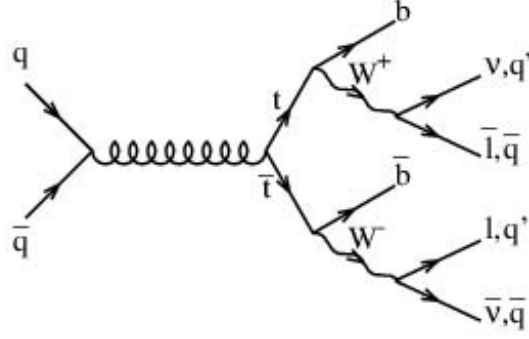


Figure 6: The LO diagram for  $t\bar{t}$  production from  $q\bar{q}$  annihilation. Each top decays into a W and a b quark, with the W decaying into leptons or quark pairs.

has two high momentum b quark jets. In contrast, directly produced W's only have b quark jets in a few percent of the events. Requiring a b-tagged jet improves the signal to background ratio from 1/4 to 3/1. The dominant backgrounds in the b-tagged sample are from  $Wbb$ ,  $Wcc$  and  $Wc$  production where either the b or charm jet is tagged. There is also background from W plus light quark production, where a light quark jet is mis-tagged due to tracking resolution. Another background is direct QCD production of jets (including b quark jets) with large missing transverse momentum due to mismeasurement, and a fake lepton or isolated lepton from b hadron decays. Additional backgrounds come from WW, WZ and single top production, which have a high  $p_T$  isolated lepton and a neutrino from W decay, along with a bottom or charm quark jet in the event.

### 3.2. Event Reconstruction and Template Mass Measurement

To fully reconstruct the  $t\bar{t}$  event in the lepton plus jets mode requires four jets to match the two b quark jets and the two quark jets from the hadronic W decay. The selection cuts for the fourth jet are often loosened to the requirement of a jet with  $E_T > 8$  GeV. In addition, we need to account for the momentum of the neutrino. We use momentum conservation to infer the neutrino momentum in the transverse direction based on the energy balance measured in the calorimeter, as is done for the W mass measurement. However, the neutrino momentum along the z direction is unknown due to the unknown momentum of the proton and anti-proton remnants that scatter at low angles. In this case we can use the known W mass to solve for the neutrino  $p_z$ , given the measured charged lepton momentum and the inferred neutrino momentum in the transverse direction. However, the neutrino  $p_z$  can only be solved up to a 2-fold ambiguity.

The other part of the event reconstruction is assigning jets to the partons from the top and W decays. With four jets there are 12 possible jet-parton assignments, where we don't distinguish between the two jets assigned to the W decay. With one or two b-tagged jets the combinatorics reduces to 6 or 2 respectively.

To reconstruct the top quark mass requires the best jet-parton assignment and neutrino momentum measurement. We use the five constraints of momentum balance in the x and y directions, the known W mass for both the hadronic and leptonic W decays and the equivalence of the two top quark masses. These constraints are used in a  $\chi^2$  to kinematically fit for the top quark mass for the different parton assignments for the event. This  $\chi^2$  is given in Equation 2 and includes constraints on the lepton and jet  $E_T$ 's based on the lepton and jet energy resolutions. The constraint using momentum balance is reflected in the constraint on the unclustered energy in the event. The unclustered energy in the event for the x and y directions, along with the lepton and jet transverse momenta are used to infer the transverse neutrino momentum. The parton-jet assignment with the lowest  $\chi^2$  is the one chosen and the top mass returned from the fit is the reconstructed mass for that event.

$$\chi^2 = \sum_{i=l,jets} \frac{(p_t^{i,meas} - p_t^{i,fit})^2}{\sigma_i^2} + \sum_{j=x,y} \frac{(p_j^{UE,meas} - p_j^{UE,fit})^2}{\sigma_j^2} \quad (2)$$



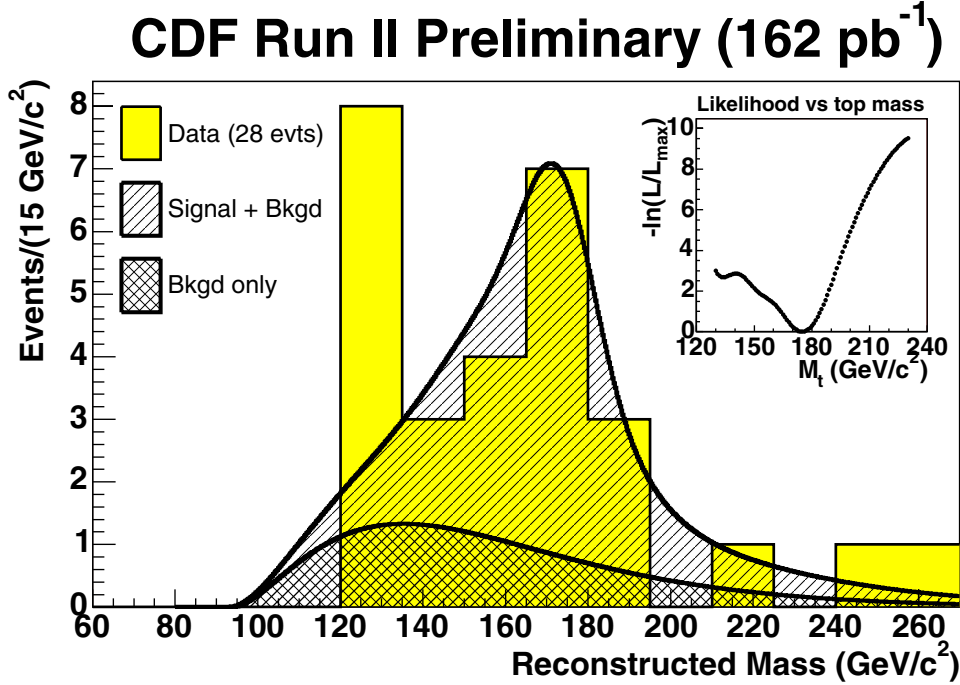


Figure 7: The reconstructed top mass distribution and associated likelihood fit for the top quark mass. This measurement is based on the template method which reconstructs the top mass using a kinematic fit.

$$\begin{aligned}
& + \frac{(M_{jj} - M_W)^2}{\Gamma_W^2} + \frac{(M_{lv} - M_W)^2}{\Gamma_W^2} \\
& + \frac{(M_{bjj} - M_{fit})^2}{\Gamma_t^2} + \frac{(M_{blv} - M_{fit})^2}{\Gamma_t^2}
\end{aligned}$$

To measure the top quark mass requires understanding how the distribution of reconstructed masses depends on the true top quark mass. In addition, the reconstructed mass depends on how often the correct jet-parton assignment was selected, how often one of the four leading jets was actually from initial or final state gluon radiation, and how the reconstructed jet energies relate to the true top quark mass. A detailed MC simulation is used to generate templates of reconstructed mass for a range of top quark masses. This set of templates is fit to parameterize how the reconstructed mass depends on the actual top quark mass. This parameterization is used in a likelihood fit to the reconstructed mass in the data. The likelihood also includes background shape templates which are obtained from MC samples and the background normalization is constrained to a background estimate based on the top cross section measurement.

The template method was used for the initial Run I top mass measurements. CDF measured a top mass of  $176.1 \pm 5.1(\text{stat}) \pm 5.3(\text{syst}) \text{ GeV}/c^2$  [15] and D0 measured a mass of  $173.3 \pm 5.6(\text{stat}) \pm 5.5(\text{syst}) \text{ GeV}/c^2$  [16]. A preliminary CDF Run 2 measurement based on  $162 \text{ pb}^{-1}$  gives a result of  $174.9_{-7.6}^{+7.1}(\text{stat}) \pm 6.5(\text{syst}) \text{ GeV}/c^2$ . This analysis had 28 events with an estimated background of  $6.8 \pm 1.2$  background events. The reconstructed mass distribution and likelihood fit is shown in Figure 7.

### 3.3. Matrix Element Methods

Several limitations of the template method are that only one permutation of parton-jet assignments is chosen, which is not always the correct one; and the jet energy constraint in the kinematic fit is parameterized with a Gaussian which does not properly handle tails in the calorimeter energy response. An improved approach to the top mass measurement is using the  $t\bar{t}$  matrix element to form an event based likelihood as a function of the top mass.

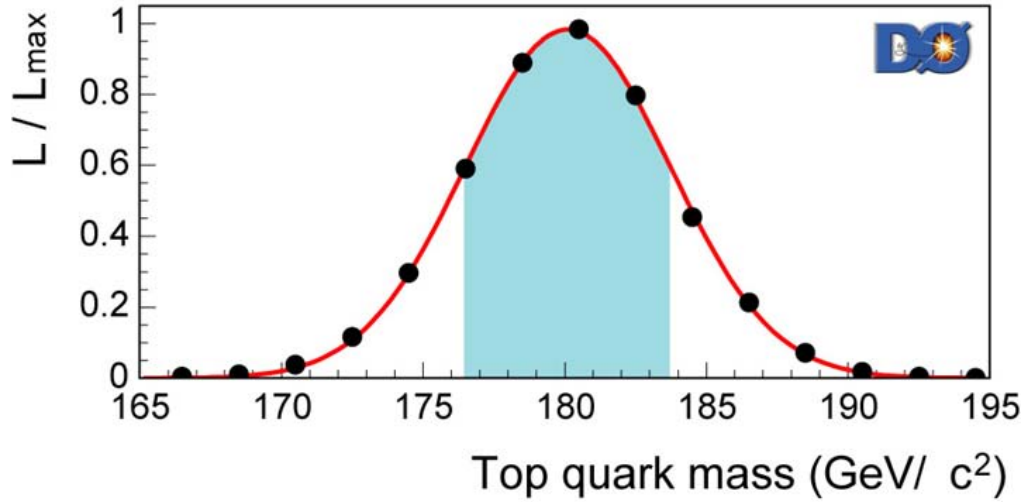


Figure 8: The D0 top mass measurement using a matrix element method. This result is based on Run I data.

This likelihood is written as

$$P(x, m_t) = \frac{1}{\sigma(m_t)} \int d\sigma(y, m_t) dq_1 dq_2 f(q_1) f(q_2) W(x, y) \quad (3)$$

where  $x$  are the observed jet and lepton energies and directions;  $d\sigma(y, m_t)$  is the differential cross section for the true parton energies and directions,  $y$ , given a top quark mass  $m_t$ ;  $f(q_1)$  and  $f(q_2)$  are the parton distribution functions; and  $W(x, y)$  is a transfer function which maps the parton level energies  $y$  to the reconstructed jet energies  $x$ . The transfer function for the lepton and the jet directions are taken to be delta functions. The transfer function for the jet energies is derived from MC simulations and allows for a non-gaussian calorimeter response. This probability as written is for a single parton-jet assignment. For the likelihood fit, all of the jet-parton assignments are used for each event and their probability distributions are summed.

This approach of using the matrix element and all of the information in the event was first proposed by K. Kondo of CDF as the Dynamic Likelihood Method (DLM) [17]. However, the first application of the method was by the D0 collaboration to their Run 1 data [18]. They used a sample of 22 lepton plus jet events without b-tagging. Included in the likelihood was the differential cross section for the W+four jet background. They obtained a result of  $180.1 \pm 3.6(\text{stat}) \pm 3.9(\text{syst}) \text{ GeV}/c^2$ . This result supersedes the D0 Run 1 template result given above and the reduction in statistical error from 5.6 to 3.6  $\text{GeV}/c^2$  is equivalent to the improvement that would be obtained with a dataset 2.4 times larger and illustrates the statistical power of the method. This measurement is shown in Figure 8.

CDF has made a preliminary measurement of the top mass using the Dynamic Likelihood method with Run 2 data. This matrix element technique has a few differences from the D0 measurement. One is that the  $p_T$  of the  $t\bar{t}$  system is included in the likelihood. This is a higher order effect due to initial state radiation of the incoming partons. The second is that there is no matrix element for background processes. That is because the CDF measurement uses a b-tagged sample with significantly less background. However, it does require a correction to the fit result to account for the effect of background. With an integrated luminosity of  $162 \text{ pb}^{-1}$ , CDF obtains a preliminary result of  $177.8^{+4.5}_{-5.0}(\text{stat}) \pm 6.2(\text{syst}) \text{ GeV}/c^2$ . This comes from a sample of 22 b-tagged lepton plus jet events with exactly four jets and an estimated background of  $4.2 \pm 0.8$  events. Figure 9 shows the maximum likelihood mass for this result.

### 3.4. Systematic Errors and Jet Energy Scale

Although the top mass measurements are made with samples of only 20-30 events, the statistical uncertainty is already less than the systematic errors. With the increasing luminosity for Run 2, the statistical error will readily

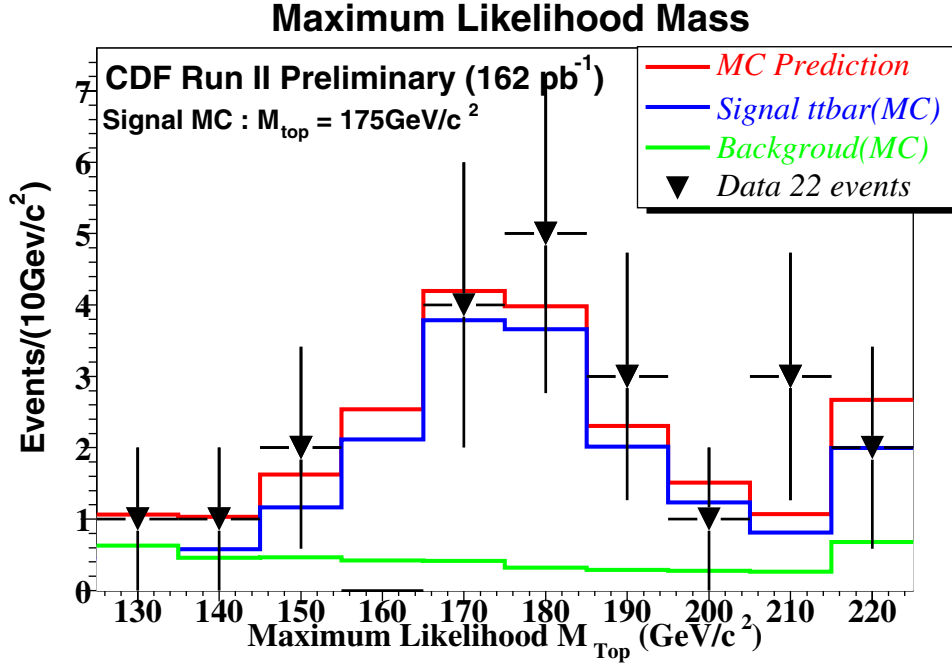


Figure 9: The maximum likelihood mass from the CDF DLM result. The signal MC is for a top quark mass of 175 GeV/ $c^2$ .

decrease and the measurement will be entirely systematics limited. Table II shows the systematic errors from the CDF DLM result (the systematic errors for the template method are similar).

The systematic error is entirely dominated by the jet energy scale. This includes understanding the calorimeter response to charged and neutral particles, non-linearity in the calorimeter response and accounting for uninstrumented regions of the detector. In addition is calibrating the absolute energy scale and correcting from the jet level measurement to the parton energy before fragmentation and hadronization. The calorimeter is calibrated with photon plus jet events,  $Z \rightarrow ee$  decays, single tracks pointing at calorimeter towers, the ratio of calorimeter energy to track momentum ( $E/p$ ) for electrons, and initial calibrations using test beam data. MC simulations are used for correcting the measured jet energy back to the parton level energy. This must take account of parton level energy that falls outside the reconstructed jet cone. Understanding these corrections requires a careful calorimeter simulation with good agreement between data and MC distributions.

Ideally a known resonance decaying to two jets would be used for calibrating the jet energy scale. However, because of the large QCD jet background, these cannot be identified in the dijet data. The  $W \rightarrow q\bar{q}$  decay in the  $t\bar{t}$  sample itself does provide a resonance decaying to two jets. In this case the known  $W$  mass is used to check the jet energy scale. With the current level of statistics, this method currently serves as a cross check, although it will become useful with larger datasets. However, the jet energy response for charm and light quark jets is not the same as the  $b$  quark jets in the top decay. One approach being pursued is to use a sample of  $Z \rightarrow b\bar{b}$  events. Requiring both jets in the event to be  $b$ -tagged provides enough reduction in background to observe the  $Z$  events on top of the large QCD background. The additional challenge in this approach is having an efficient trigger to select  $b$  jet events. At CDF this is done by selecting a displaced vertex in a jet at the trigger level.

### 3.5. Additional Top Mass Measurements

Another approach to measuring the top quark mass in the lepton plus jets channel uses the  $W \rightarrow q\bar{q}$  decay in the top event to fit for the jet energy scale while measuring the top mass. This represents a tradeoff between the statistical and systematic error which in the limit of high statistics will give an overall improved measurement. This

Table II: Systematic errors for the CDF DLM top mass measurement.

Source	$\Delta M_{top}$ GeV/ $c^2$
Jet Energy Corrections	5.3
ISR	0.5
FSR	0.5
PDFs	2.0
Generator	0.6
Spin correlation	0.4
NLO effect	0.4
Transfer Function	2.0
Background fraction ( $\pm 5\%$ )	0.5
Background Modeling	0.5
Monte Carlo Modeling	0.6

CDF analysis is referred to as the Multivariate Template method (MTM) and is an extension of the template method described earlier. In addition, this method uses the  $E_T$  sum of the four leading jets as a way to distinguish signal and background, and includes the background fraction as a parameter in the fit. With a  $162 \text{ pb}^{-1}$  dataset, this method has a preliminary result of  $179.6^{+6.4}_{-6.3}(\text{stat}) \pm 6.8(\text{syst}) \text{ GeV}/c^2$  for the top quark mass and measures a background fraction of  $0.35 \pm 0.14$  for a sample of 33 events.

The standard template method has also been applied to the untagged lepton plus jets sample. In this case the four jets are required to have  $E_T > 21 \text{ GeV}$  to reduce the W plus jets background. With a dataset of  $193 \text{ pb}^{-1}$ , CDF has 39 candidate events with an estimated background of  $15.5 \pm 3.2$  events. The top quark mass is measured to be  $179.1^{+10.5}_{-9.5}(\text{stat}) \pm 8.4(\text{syst}) \text{ GeV}/c^2$ . Although this measurement is not as precise as the one using the tagged sample, it is statistically independent and can be combined with the tagged sample to reduce the overall error.

The top quark mass can also be measured in the dilepton mode where both of the W's in the event decay to an electron or muon. This sample requires two leptons with transverse momentum above  $20 \text{ GeV}/c$ , a transverse momentum imbalance above  $25 \text{ GeV}/c$ , and two or more jets with  $E_T > 15 \text{ GeV}$ . Because of the two undetected neutrinos in the event, the kinematics is underconstrained and the event cannot be fully reconstructed. A  $t\bar{t}$  MC sample is used to give a probability distribution for the  $p_z$  of the  $t\bar{t}$  system, effectively giving the final constraint needed for the mass measurement. A preliminary CDF result with  $126 \text{ pb}^{-1}$  of data has six candidate events with an expected background of  $0.5 \pm 0.2$  events. This analysis measures a top quark mass of  $175.0^{+17.4}_{-16.9}(\text{stat}) \pm 8.4(\text{syst}) \text{ GeV}/c^2$ . Although this measurement is statistically limited, using the dilepton sample gives an independent measurement with a different set of systematic errors and very different backgrounds.

## 4. CONCLUSIONS

Precision measurements of both the W boson and top quark masses can be combined with other electroweak observables to put constraints on new physics and place a bound on the Higgs mass.

The combined CDF and D0 Run I W mass measurement has a total uncertainty of  $60 \text{ MeV}/c^2$ . With increasing datasets with Run 2, the statistical uncertainty will continue to decrease. The dominant systematic uncertainties are largely based on the  $Z \rightarrow \ell\ell$  calibration samples. As the size of this sample grows, the systematic uncertainties will also be reduced. The Run 2 goal of an uncertainty of  $40 \text{ MeV}/c^2$  per experiment for  $2 \text{ fb}^{-1}$  of data should be achievable.

The use of matrix element based methods for the top mass measurement has produced the best Run 1 measurement of the top mass and gives the most precise Run 2 measurement from CDF. However, the top mass measurement is already systematics limited and much improvement will be needed on understanding the jet energy scale. The goal

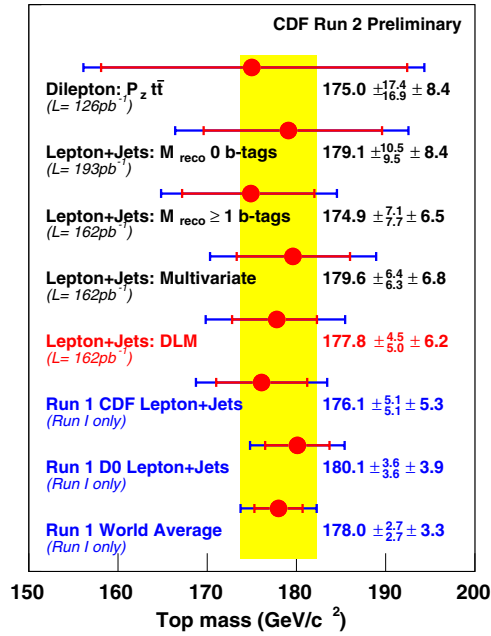


Figure 10: A summary of recent CDF and D0 top mass measurements.

for Run 2 is a measurement of the top mass with an uncertainty of  $3 \text{ GeV}/c^2$  per experiment. A listing of several recent CDF and D0 top mass measurements is shown in Figure 10, along with the Run 1 averages.

## Acknowledgments

The author wishes to thank the D0 and CDF collaborations for the results presented in this talk, and the Fermilab accelerator division for the operation of the Tevatron collider.

## References

- [1] W. J. Marciano, "Precision Electroweak Measurements and the Higgs Mass", XXIII SLAC Summer Institute 2004, hep-ph/0411179
- [2] CDF Collaboration, D. Acosta *et al.*, Phys. Rev. D **71**, 032001 (2005)
- [3] D0 Collaboration, V. Abazov *et al.*, in preparation for submission to Nucl.Instrum. Methods Phys. Res. A.
- [4] D0 Collaboration, B. Abbot *et al.*, Phys. Rev. D **58**, 092003 (1998)
- [5] D0 Collaboration, V. M. Abazov *et al.*, Phys. Rev. D **66**, 012001 (2002)
- [6] CDF Collaboration, T. Affolder *et al.*, Phys. Rev. D **4**, 52001 (2001)
- [7] C. Balazs and C.-P. Yuan, Phys. Rev. D **56**, 5558 (1997).
- [8] G. A. Ladinsky and C.-P. Yuan, Phys. Rev. D **50**, 4239 (1994).
- [9] R. K. Ellis and S. Veseli, Nucl. Phys. **B511**, 649 (1998).
- [10] F. A. Berends and R. Kleiss Z. Phys. C **27**, 365 (1985); F. A. Berends *et al.*, *ibid.* **27**, 155 (1985).
- [11] E. Barberio and Z. Was, Comput. Phys. Commun. **79**, 291 (1994).
- [12] U. Baur, S. Keller, and D. Wackeroth, Phys. Rev. D **59**, 013002 (1999).

- [13] A. D. Martin *et al.*, Eur. Phys. J. **C23**, 73 (2002).
- [14] J. Pumplin *et al.*, JHEP 0207 (2002); H. L. Lai *et al.*, Phys. Rev. D **51**, 4763 (1995).
- [15] CDF Collaboration, T. Affolder *et al.*, Phys. Rev. D **63**, 032003 (2001)
- [16] D0 Collaboration, B. Abbot *et al.*, Phys. Rev. D **58**, 052001 (1998)
- [17] K. Kondo, J. Phys. Soc. **57**, 4126 (1988)
- [18] D0 Collaboration, V. M. Abazov *et al.*, Nature **429**, 638 (2004).